Research Article | Vol. 24, No. 20 | 3 Oct 2016 | OPTICS EXPRESS 23018

Optics EXPRESS

Structured illumination behind turbid media

A. MALAVALLI, M. ACKERMANN AND C. M. AEGERTER*

Physics Institute, University of Zurich, Winterthurerstrasse 190, 8057 Zurich, Switzerland
*aegerter@physik.uzh.ch

Abstract: In turbid media, light gets multiply scattered to an extent that all the information of its propagation is scrambled over a characteristic distance called the transport mean free path. Controlling light propagation through such media is therefore challenging. By using a feedback signal, the input wavefront of light can be shaped such that light gets focused through or even inside a scattering medium [Vellekoop et al., Opt. Express *36*, 67 (2008)]. In this article, we show that such an interferometric focus can be transformed into an array of multiple focal spots with a desired structure. These focal spots can serve as a structured illumination source to image the interior of thick scattering tissues as in deconvolution imaging or in the optical micromanipulation of microscopic targets.

OCIS codes: (110.0113) Imaging through turbid media; (110.2945) Illumination design; (120.5060) Phase modulation

References and links

1. I. M. Vellekoop and A. P. Mosk,"Focusing coherent light through opaque strongly scattering media," Opt. Lett. **32**(16), 2309–2311 (2007).
2. I. M. Vellekoop, E. G. van Putten, A. Lagendijk, and A. P. Mosk,"Demixing light paths inside disordered metamaterials", Opt. Express **16**(1), 67–80 (2008).
3. C. Maurer, A. Jesacher, S. Fürhapter, S. Bernet and M. Ritsch-Marte, "Tailoring of arbitrary optical vector beams", New J. Phys. **9**(78), 1367–2630 (2007).
4. B. Chang, L.Chou, Y. Chang and S. Chiang,"Isotropic image in structured illumination microscopy patterned with a spatial light modulator," Opt. Express **17**(17), 14710–14721 (2009).
5. M.G.L. Gustafsson. "Surpassing the lateral resolution limit by a factor of two using structured illumination microscopy," J. Microsc. **198**, 82–87 (2000).
6. M. A. A. Neil, R. Juskaitis, and T. Wilson, "Method of obtaining optical sectioning by using structured light in a conventional microscope," Opt. Lett. **22**(24), 1905–1907 (1997).
7. S. W. Hell, & J. Wichmann, "Breaking the diffraction resolution limit by stimulated emission: stimulated-emission-depletion fluorescence microscopy," Opt. Lett. **19**, 780–782 (1994).
8. C. Kuang, S. Li, W. Liu, X. Hao, Z. Gu, Y. Wang, J. Ge, H. Li & X. Liu,"Breaking the Diffraction Barrier Using Fluorescence Emission Difference Microscopy," Sci. Rep. **3**, 1441 (2013).
9. T. Čižmár & K. Dholakia,"Shaping the light transmission through a multimode optical fibre: complex transformation analysis and applications in biophotonics," Opt. Expres, **19**(20), 18871–18884 (2011).
10. T. Čižmár, M. Mazilu and K. Dholakia,"In situ wavefront correction and its application to micromanipulation," Nat. Photon. **4**, 388–394 (2010).
11. S. Bianchia and R.Di Leonardo, "A multi-mode fiber probe for holographic micromanipulation and microscopy," Lab Chip **12**, 635–639 (2012).
12. S. Popoff, G. Lerosey, M. Fink, A. C. Boccara & S. Gigan,"Image transmission through an opaque material," Nat. Commun. **1** 81 (2010).
13. I.M.Vellekoop, "Feedback-based wavefront shaping," Opt. Express **23**(9), 12189–12206 (2015).
14. G. Ghielmetti and C.M. Aegerter,"Scattered light fluorescence microscopy in three dimensions," Opt. Express **20**(4), 3744–3752 (2012).
15. I. M. Vellekoop, A. Lagendijk, and A. P. Mosk,"Exploiting disorder for perfect focusing," Nat. Photon. **4**, 320–322 (2010).
16. T. Chaigne, J. Gateau, O. Katz, E. Bossy, and S. Gigan, "Light focusing and two-dimensional imaging through scattering media using the photoacoustic transmission matrix with an ultrasound array," Opt. Lett. **39**(9), 2664–2667 (2014).
17. I.M. Vellekoop & A.P. Mosk, "Phase control algorithms for focusing light through turbid media," Opt. Commun. **281**, 3071–3080 (2008).
18. G. Ghielmetti and C. M. Aegerter,"Direct imaging of fluorescent structures behind turbid layers," Opt. Express **22**(2), 1981–1989 (2014).
19. I.M.Vellekoop, Doctoral dissertation "Controlling the propagation of Light in Disordered Scattering Media".
20. D. Engström, A. Frank, J. Backsten, M. Goksör, and J. Bengtsson, "Grid-free 3D multiple spot generation with an efficient single-plane FFT-based algorithm," Opt. Express **17**(12), 9989–10000 (2009).

#272460 http://dx.doi.org/10.1364/OE.24.023018
Journal © 2016 Received 3 Aug 2016; revised 16 Sep 2016; accepted 18 Sep 2016; published 26 Sep 2016

Optics EXPRESS

21. J. W. Goodman, *Statistical Optics* (Wiley, 2000).
22. I. Freund, M. Rosenbluh, and S. Feng, "Memory Effects in Propagation of Optical Waves through Disordered Media," Phys. Rev. Lett. **61**, 2328–2331 (1988).

1. Introduction

Wavefront shaping is gaining much attention in the field of light microscopy to control the propagation of light in multiply scattering materials [1, 2]. It is one of the ways to counter the effects of scattering when imaging through materials of biological interest. Wavefront shaping has also been used to structure the illumination pattern in light microscopy. Interference between multiple orders of diffraction from a grating forms a sinusoidally varying light field. First order Bessel modes or other higher order vector modes can be generated using Spatial Light Modulators (SLM) [3, 4]. Such synthetic illumination patterns are known to enhance resolution in imaging beyond the diffraction limit [4–6] and Bessel or donut beams have been used for excitation-deexcitation beam configurations in STED microscopy [7, 8]. However, when transmitting these illumination patterns through turbid media, light gets multiply scattered and the pattern is quickly lost. Hence, structured illumination approach is able to work with optically thin or transparent sections, which is often limited to superficial layers of samples.

Using SLMs, the wavefront of incoming light can be modulated in phase and amplitude in order to control the scattered light field. In adaptive optics, feedback based algorithms are used to correct for abberations from optical setups and to map the transmission matrix of abberated systems such as optical fibers [9]. This approach has been widely used for trapping and micromanipulation of particles [10, 11]. But mapping such a transmission matrix can be time consuming when many configurations of output fields are to be realised [12]. It is however now possible to focus light through a multiply scattering medium using feedback based algorithms [13] and scan this focus in 3D [14]. In the present article we extend this technique to obtain multiple focal spots behind a multiply scattering medium.

The working principle of our technique as demonstrated by Fig. 1 is that a diffraction limited focus can be generated using a feedback based technique using an iterative algorithm [15–17] and such a focus can then be transformed into a user defined configuration of multiple focal spots. After the optimization process, the scattering medium acts as a turbid lens that focuses the spatially modulated optimum wavefront. By adding a desired phase mask to this wavefront, multiple focal spots can be generated by virtue of convolution theorem. As this technique does not depend on the type of feedback mechanism used to create the initial focus it can be beneficial especially when a direct access to the focal plane is not available [18]. The theory concerning this technique is decribed in section 2. The computation of such phase masks, also called Computer Generated Holograms (CGHs) is described in section 3 followed by the experimental results in section 4. Multiple foci can also be generated without the use of these CGHs- by directly

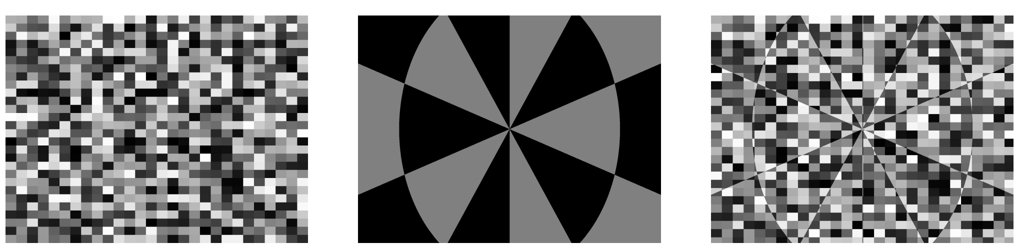

a) Optimum Wavefront b) Computed CGH c)Final SLM phase

Fig. 1. To the optimum wavefront a) leading to a focus behind the turbid medium, when a CGH such as b) is added, the resulting phase would look like c).

Optics EXPRESS

optimizing on multiple targets as previously described in [19]. In section 5 of this article we further describe and compare these methods.

2. Theoretical background

As shown in the experimental setup Fig. 2, the SLM plane and sample form conjugate planes such that an image of the SLM screen is formed on the sample. When a phase modulation scheme is used [17], the computer algorithm iteratively alters the phase of the pixels on the SLM to form an interferometric focus at the focal plane.

After focusing, the combination of SLM and the scattering medium acts as a lens. If the beam coming into the SLM is tilted, the focal spot moves. This tilting effect can also be implemented by just adding a suitable phase to the modulated wavefront at the SLM. The same works if we add a phase pattern that, like a grating, results in multiple beams. To this combination resulting in a lens, by adding the phase pattern of a grating, we bring the far field of the grating onto the focal plane, resulting in multiple spots.

If $\mathcal{E}_i = \mathcal{E}_0 \exp^{i\,\phi}$ is the electric field of the wavefront with phase ϕ modulated by the SLM to obtain a focus, the field at the focal plane on the CCD is given by [14],

$$\mathcal{E}_f = \iint\limits_S \mathcal{E}_i \, t_{i\,s} \, g(r_f - r_s) \, d^2 r_s \tag{1}$$

integrated over the scattering plane of the sample. Here, $t_{i\,s}$ is the coefficient of the optical setup for transmitting light from each segment of the SLM to the output plane of the sample and the light propagaion from this plane to the CCD is described by the free space Green function $g(r_f - r_s)$ [15]. It has been shown experimentally [15] that the shape of this interferometric focus is same as the speckle correlation function [21].

Transformation of this focus into multiple foci can be understood using the convolution theorem. It states that,

if $\mathcal{F}\{\mathcal{E}_f(y,z)\} = E(k_y, k_z)$ and $\mathcal{F}\{f(y,z)\} = F(k_y, k_z)$, then

$$\begin{aligned} \mathcal{F}\{\mathcal{E}_f * f\} &= \mathcal{F}\{\iint\limits_{-\infty}^{+\infty} \mathcal{E}_f(y,z)\, f(Y-y, Z-z)\, dy\, dz\} \\ &= \mathcal{F}\{\mathcal{E}_f(y,z)\}\ \mathcal{F}\{f(y,z)\} \\ &= E(k_y, k_z)\ F(k_y, k_z) \end{aligned} \tag{2}$$

i.e if $\mathcal{E}_f(y,z)$ represents the field distribution of the interferometric focus and $f(y,z)$ represents Dirac delta functions with their peaks located where the focal spots are desired,

$$f(y,z) = \sum_i \exp^{i\,\phi_i} \delta(y - y_i)\delta(z - z_i) \tag{3}$$

the convolution between the two leads to a multiple focal pattern in the image plane. Furthermore, the phase that needs to be added on the SLM plane in order to obtain this multiple focal pattern can be extracted by noticing that,

$$E(k_y, k_z) = \mathcal{E}_i \, t_{i\,s} \, g(r_f - r_s) \tag{4}$$

and as $t_{i\,s}$ and $g(r_f - r_s)$ are unaffected, $\mathcal{F}\{\mathcal{E}_f * f\} = \mathcal{E}_i \, F(k_y, k_z)$

Since we make use of phase only modulation scheme, the intensity contribution to the focal plane from different regions of sample is not the same, leading to fluctuations in intensity when focal spots move. However this could be rectified if both phase and amplitude modulation scheme were used in the optimization process.

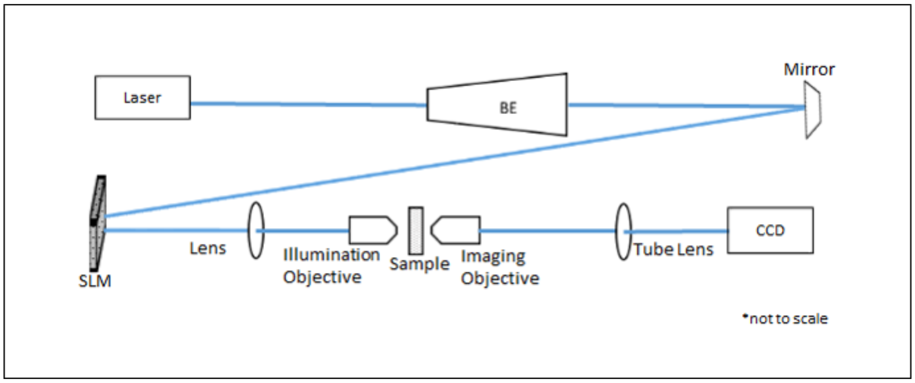

Fig. 2. Experimental Setup.

3. Experimental setup

The experimental setup is as shown in Fig. 2. Light from a Cyan laser (Newport Spectra-Physics) at 488nm is expanded with a beam expander setup (BE) to fill the screen of the SLM (HOLOEYE HEO 1080P). The SLM plane is imaged onto the sample using a lens and a 40x illumination objective, such that the SLM and the sample make a pair of conjugate planes. The back surface of the sample is imaged with a 50X objective and a CCD. We made use of opaque samples of microscope slide coated with TiO_2 with thicknesses ranging from 3-15μm. Light transmitted through such a sample is multiply scattered and forms a speckle pattern on the CCD. Using stepwise sequential algorithm [17], the SLM modulates the phase of the input wavefront while monitoring the intensity enhancement at a small target region (typically about the size of a single speckle) on the CCD. The input intensity before optimisation is kept low enough to avoid saturation on the CCD. After iterating over the whole SLM, an interferometric focus is formed at the target. Once this initial focus is formed, the CGHs can be loaded onto the optimized wavefront on the SLM plane and the resulting multiple foci can be visualised on the CCD. Using linear or parabolic phase gradients at the SLM, the focal spots can be translated on the CCD. For the experiments involving movement of the foci, a grit polished diffuser glass was used as a sample.

4. Phase mask generation

The generation of CGHs is a crucial step of these experiments. Depending on the complexity of the desired configuration of focal spots, one can choose from different methods to generate the CGH [3, 20]. As the Fourier transformation operation is reversible [22], the phase modulation by $F(k_y, k_z)$, as described in Eq. (2-3), in the scattering plane of the sample should lead to a 2D grid of Dirac delta functions in the image plane, as described in the previous section. To get a planar grid of equally spaced focal spots, we generated grayscale images such as shown in Fig. 3(a). The phase modulation is achieved using 8-bit bitmap images, whose grayscale values between 0-255 correspond to a phase modulation between 0-2π. These images constitute a combination of binary gratings of multiple periods extending in 2 dimensions. Furthermore, we computed the Fourier transform of the phase values of these images to verify that the intensity peaks in the image plane appear at the spatial frequencies defined by the periodicity of the gratings. These peaks in the Fourier transform correspond to the positions of the focal spots that would be formed on the image plane Fig. 3(b). The grayscale values and/or the period of the gratings in the images were altered to change the configuration and position of the spots in the Fourier plane. The smaller the period is, the farther away the spots move in Fourier space Fig. 4. In this manner

Optics EXPRESS

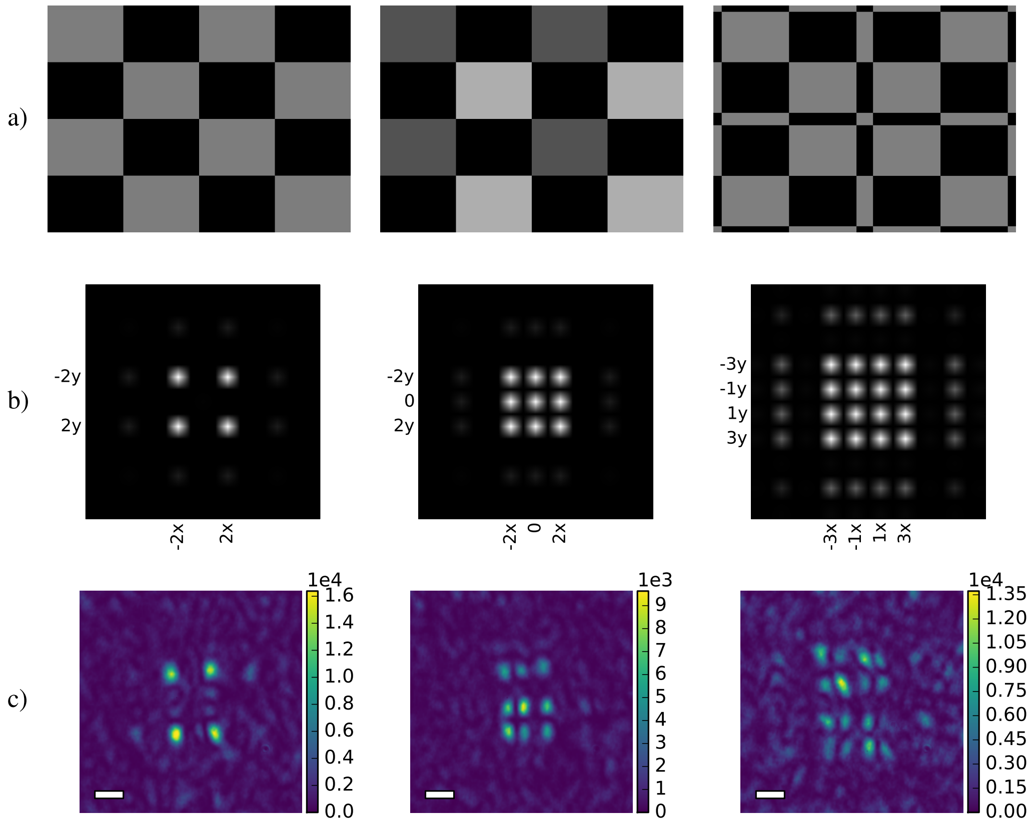

Fig. 3. a) Phase masks loaded onto the SLM for obtaining multiple focal spots through a layer of TiO_2 b) computed Fourier Transforms of (a). c) resulting pattern on the CCD for respective images in (a). Scalebar corresponds to 5μm.

we are able to generate different configurations of focal spots with rectangular as well as radial symmetry Fig. 5.

We have also used two algorithms that try to generate optimal phase masks. These algorithms simulate an SLM plane where the field is modulated such that when Fourier Transformed, the intensity is enhanced at certain predefined locations. The first approach is a genetic algorithm that optimizes the phase of the rectangular regions of the SLM. It works with a population of phasemasks, where each phasemask has phase values for each rectangular region. Through mutations and inheritance, the population evolves towards an optimal solution. For the second approach, we set the phase mask to $\phi(\text{y}, \text{z}) = \arg(\text{ifft}(\text{F}))$ where F is zero everywhere except at the target spots and ifft corresponds to inverse Fourier transform operation. If we calculate F from $\phi(y, z)$ as described in section 2, then the central spots will have a much lower intensity than those at the edges Fig. 6. This is caused by taking the argument of the ifft which drops all intensity information of our spectrum. We can regain uniformity by optimizing the phase of the spots in F using stochastic optimization. Both algorithms result in multiple focal spots being formed on the image plane as shown in Fig. 6.

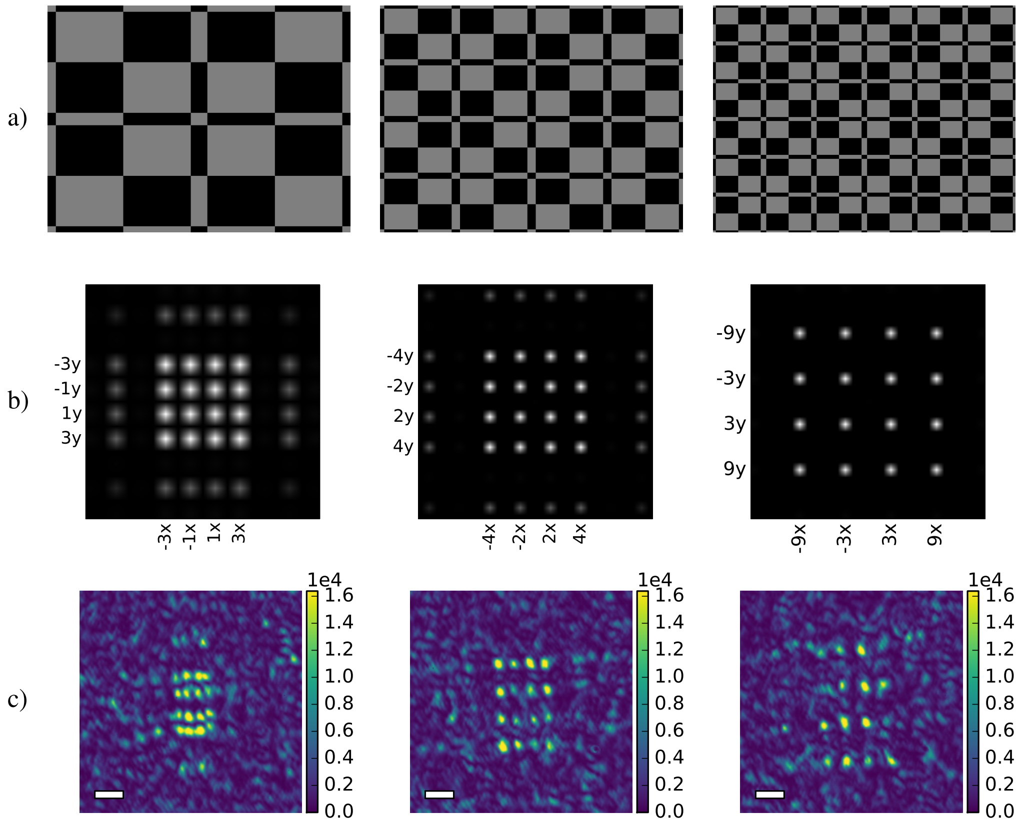

Fig. 4. Moving the focal spots in k-space: a) the SLM masks. b) computed Fourier Transforms c) resulting CCD images for diffuser glass used as sample. Scalebar corresponds to 5μm.

5. Results and discussion

The CGHs such as those described in the previous section can be generated independently of the real time experiments beforehand. In the real time experiments, once the interferometric focus is obtained, these CGHs can be added to the SLM and the resulting multiple foci can be visualised on the CCD. We demonstrate some sample configuration of focal spots which are formed by the respective CGHs as shown in Fig. 3 through 7.

Thus created multiple focal spots can be in turn used to illuminate–for example–flourescent targets in biological samples and image them. The ability to realise any configuration of focal spots can make it easier to acquire sample information from multiple locations parallely. It could also be possible to optically trap and micro manipulate targets hidden within turbid media, which would otherwise be inaccessible. The simplicity of the approach of Fourier transformation makes it easier to translate and rotate the focal spots. By adding a linear phase shift to the phase masks in the SLM plane, we are able to translate the spots. Similarly, a parabolic phase shift would move the spots in the forward direction out of the plane [4]. Also, when the coordinate axes of the images are rotated, the focal spots follow the drift and rotate in the image plane. (see Visualization 1). This freedom of moving the focal spots can accelerate image acquision process compared to raster scanning a single focal spot.

Translating the foci however depends on the range of memory effect [22], defined as the extent to which the transmitted light preserves the information about the input phase and amplitude

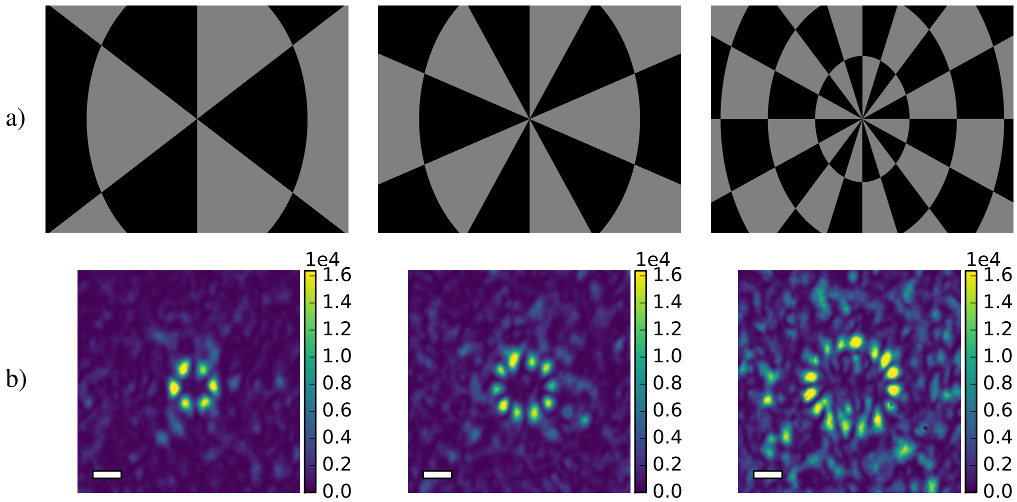

Fig. 5. a) Phase masks loaded onto the SLM to obtain focal spots with radial symmetry. b) Resulting patterns on the CCD respectively. Scalebar corresponds to 5μm.

variation. The memory effect range falls as the inverse of the thickness of the medium. For a thick 15μm layer of TiO_2, it is about 3μm and the pattern of multiple foci is lost when translated further than this range. This is also the case when the distance between the focal spots is more than the range of memory effect. Hence such experiments can only be perfomed on optically thin samples. Figure 4 shows the possibility of movement of focal spots through a diffuser for which memory effect range is theoretically unlimited [22]].

Although, the size and shape of the initial focus is retained in the multiple foci, their intensities are lower than the initial focus. Due to this, the input intensity was increased to make the focal spots visible, and thus rescaling the range of transmitted intensity on the CCD. This reduction is attributed to the intensity enhancement of initial focus with respect to the background- that gets redistributed among the multiple foci. Hence there exists a tradeoff between the contrast and the number of foci, which in turn are limited by the achievable intensity enhancement. Multiply scattering TiO_2 samples also cause this contrast to be lost quickly compared to less scattering diffuser glass. Fig. 7 demonstrates the limiting case for our signal to background ratio; where 36 focal spots are created through a diffuser, which was not possible with TiO_2 samples. Beyond this, the focal spots were indistinguishable from the background speckles in any sample.

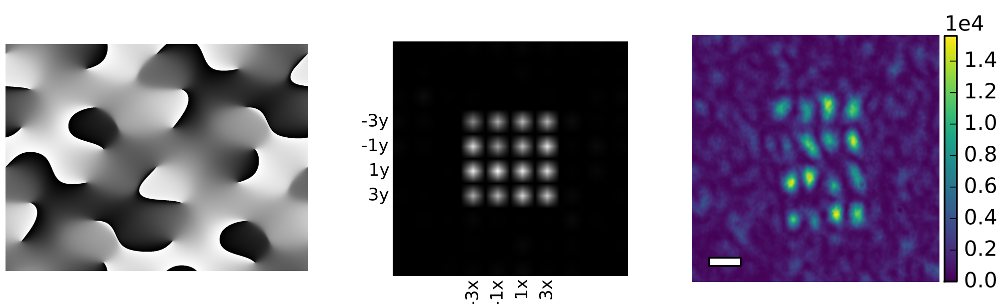

Fig. 6. CGH generated using Stochastic algorithm, computed Fourier Transform and resulting focal spots on CCD plane. Scalebar corresponds to 5μm.

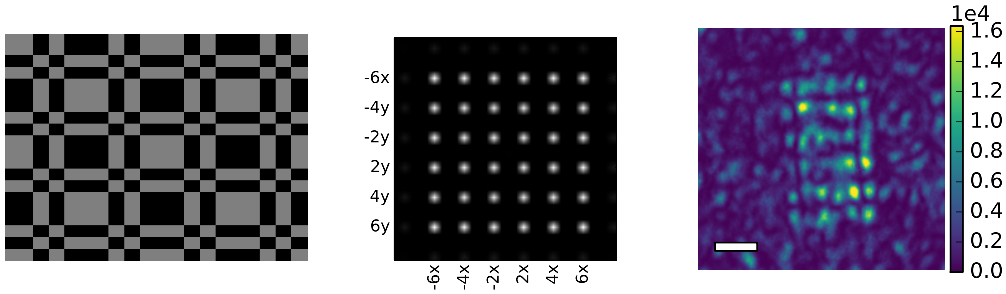

Fig. 7. Limiting case of number of foci demonstrated for diffuser glass: SLM mask,computed Fourier Transform and resulting CCD image. Scalebar corresponds to 10μm.

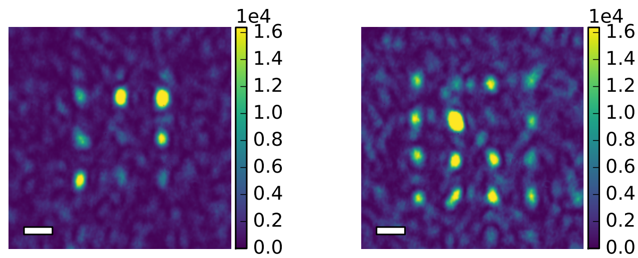

Fig. 8. Direct optimization on multiple configurations of a target. Scalebar corresponds to 5μm.

As a comparitive study to that noted previously in [19] we also perfomed the experiments by directly optimizing on multiple targets in the focal plane. We defined multiple configurations of a target Fig. 8 at the back of the sample and saw that the algorithm manages to optimize on all the targets well as long as the number of targets is small. For a large number of targets, the intensity distribution grows to be more non-uniform. This may not be desirable for applications where intensity destributions play a role. In addition, this technique by construction requires optical access to multiple locations of the focal plane and would not work well when such an access is not available.

6. Conclusion

In this article we have described a technique to obtain multiple focal spots behind a turbid medium. Computer generated phase masks can be used to transform an interferometric focus obtained behind a turbid medium into a desired configuration of multiple focal spots. With the ability of further manipulating these phase masks, the focal spots can be freely translated and rotated. This technique can find potential applications in the field of bioimaging such as structured illumination microscopy behind turbid media or optical control and micromanipulation of particles hidden in turbid environments.

Funding

Swiss National Science Foundation (Award Number 501100001711).

Optics EXPRESS

Acknowledgments

We would like to thank Dr. Jale Schneider for her contributions to the phase mask generation techniques using Genetic Algorithm.